ELSEVIER

Solid State Ionics 136–137 (2000) 305–311

SOLID STATE IONICS

www.elsevier.com/locate/ssi

Electronic transport properties and electronic structure of $InO_{1.5}$-doped $CaZrO_3$

Shu Yamaguchi[a,*], Kiyoshi Kobayashi[b], Toru Higuchi[c], Shik Shin[d], Yoshiaki Iguchi[a]

[a]*Department of Materials Science and Engineering, Nagoya Institute of Technology, Gokiso, Showa, Nagoya 466-8555, Japan*
[b]*National Institute of Materials and Chemical Research, Higashi 1-1, Tsukuba 305-8565, Japan*
[c]*Faculty of Science, Science University of Tokyo, Kagurasaka 1-3, Shinjuku, Tokyo 162-0825, Japan*
[d]*Institute of Solid State Physics, University of Tokyo, Tanashi 188-8501, Japan*

Abstract

Simultaneous measurements of total conductivity and thermoelectric power have been made on 1 mol% $InO_{1.5}$-doped $CaZrO_3$ ($CaZr_{0.99}In_{0.01}O_{0.995}$) in order to evaluate defect chemical parameters and both electronic and ionic transport properties. The concentrations of holes, protons, and oxygen vacancies and their mobility, in addition to the heat of transport of oxide ions and protons, have been estimated using defect chemical and irreversible thermochemical analyses. The present results show that the dissolution reaction of protons saturates below 1173 K and the concentration of holes decreases by the dissolution of protons, indicating the presence of direct substitution of protons with holes. O1s X-ray absorption spectroscopy has been employed to observe the electronic structure near the band gap, showing the presence of holes at the top of the valence band and the splitting of the hole state when protons dissolve. The decrease in the hole concentration observed under reducing conditions is consistent with the defect chemical analysis.

Keywords: Conductivity; Thermoelectric power; Seebeck coefficient; Mixed conductor; Proton conductor; Mobility; XAS

1. Introduction

After the discovery of perovskites with proton conductivity at elevated temperatures [1], various investigations were made to clarify its origin and nature. However, only little information is available at present on the transport properties and electronic structure of these oxides [2]. The present authors have shown that simultaneous measurements of conductivity and thermoelectric power can yield valuable information on defect chemical and transport properties, such as the concentration and mobility of charge carriers, the equilibrium constant for the defect chemical reactions, etc. [3,4]. In the previous reports, the experimental technique was applied to $CaZrO_3$ doped with 1 mol% $InO_{1.5}$ under dry conditions, where both oxide ion and hole conductivities prevail. The authors successfully estimated both the concentration and mobility of carriers. In the present study, the same experimental technique has been used to evaluate the electric transport properties of $InO_{1.5}$-doped $CaZrO_3$ ($CaZr_{0.99}In_{0.01}O_{0.995}$) under humidified conditions, where proton and hole conductivities prevail. In addition, X-ray absorption spectroscopy (XAS) was

*Corresponding author. Fax: +81-52-735-5318.
E-mail address: yamagchi@mse.nitech.ac.jp (S. Yamaguchi).

0167-2738/00/$ – see front matter
PII: S0167-2738(00)00408-2

employed to observe the electronic structure near the band gap.

2. Experimental

A sample, identical to that in the previous report [3], with nominal composition $CaZr_{0.99}In_{0.01}O_{2.995}$ was used for the measurements. The total conductivity was measured using a four-probe d.c. method under a humidified (wet) atmosphere. Thermoelectric power was measured by a two-probe method with a Pt/gas reversible electrode under the transient state condition. It was not expected to attain the Soret steady state condition, in which all the partial fluxes in the sample under a temperature gradient become zero, since the present system is a ternary one with two gaseous components. Both measurements were made simultaneously in the same cell under a fixed partial pressure of H_2O (p_{H_2O}) of 0.037 atm by varying p_{O_2} using $Ar+O_2+H_2O$ and $Ar+H_2+H_2O$ gas mixtures. The measurements were made between 1073 and 1523 K with a 50 K step. Details of the experimental procedures have been reported previously [3].

XAS measurements were carried out for samples doped with 0, 0.01, and 0.02 mol% $InO_{1.5}$ at the Photon Factory of the High Energy Accelerator Research Organization (Tsukuba, Japan). Synchrotron radiation from the undulator was monochromatized using a grating monochrometer VLM19. The resolution of the beamline was smaller than ≈ 0.1 eV at $h\nu = 500$ eV. The XAS spectra were measured by a XUV silicon photodiode. Details of the experimental procedure will be published elsewhere [5].

3. Results and discussion

3.1. Defect chemistry and theory of the Seebeck coefficient

Both ionic and hole conductivities were observed in the total conductivity measured under the present conditions. The defect chemical model employed here is identical to those proposed for other proton-conducting perovskites doped with trivalent cations [3]. The following is a summary of the defect chemical equations written in terms of the Kröger and Vink notation:

$$V_O^{\cdot\cdot} + \tfrac{1}{2}O_2 = O_O^x + 2h^{\cdot}, \tag{A}$$

$$K_{OX} = p^2/[V_O^{\cdot\cdot}](p_{O_2})^{1/2} = K_{OX}^o \exp(-\Delta H_{OX}/RT), \tag{1}$$

$$\tfrac{1}{2}H_2O + V_i + h^{\cdot} = H_i^{\cdot} + \tfrac{1}{4}O_2, \tag{B}$$

$$K_H = [H_i^{\cdot}](p_{O_2})^{1/4}/p(p_{H_2O})^{1/2} = K_H^o \exp(-\Delta H_H/RT), \tag{2}$$

where ΔH_{OX} and ΔH_H are the enthalpy changes of reactions (A) and (B), K_{OX} and K_H are the equilibrium constants for the quasi-chemical reactions (A) and (B), respectively, and K_{OX}^o and K_H^o are the so-called pre-exponential factors of the respective reactions. Square brackets indicate the concentrations of the respective defects, which are expressed by the number of defects per unit formula of $CaZrO_3$. The overall electrical neutrality condition is written as

$$2[V_O^{\cdot\cdot}] + p + [H_i^{\cdot}] = [In_{Zr}^{\prime}]. \tag{3}$$

As will be explained below, since the partial conductivity of holes (σ_p) was approximately proportional to $(p_{O_2})^{1/4}$ under the present experimental conditions, the total conductivity (σ_t) can be expressed as

$$\sigma_t = \sigma_i + \sigma_p^o(p_{O_2})^{1/4}, \tag{4}$$

where σ_p^o and σ_i are the partial conductivities of holes and ions at unit p_{O_2}. The latter is expressed by the partial conductivity of protons ($\sigma_{H_i^{\cdot}}$), oxygen vacancies ($\sigma_{V_O^{\cdot\cdot}}$), and their transference numbers ($t_{H_i^{\cdot}}$ and $t_{V_O^{\cdot\cdot}}$) as $\sigma_i = t_{H_i^{\cdot}} \cdot \sigma_{H_i^{\cdot}} + t_{V_O^{\cdot\cdot}} \cdot \sigma_{V_O^{\cdot\cdot}}$. Under wet conditions, $[H_i^{\cdot}]$ can also be approximated as being independent of p_{O_2} under fixed p_{H_2O} conditions. By the least square analysis using Eq. (4), σ_i, σ_p^o, and the transference numbers of ions and holes were evaluated for further analysis of the Seebeck coefficient.

The total Seebeck coefficient (Q_t) for mixed ionic and electronic conductors depends upon the conditions of the measurement as suggested by Wagner and various authors [6,7]. From a consideration of

the experimental results, the authors concluded that the present experimental conditions correspond to a non-Soret steady state under the attainment of a local equilibrium at electrodes between the sample and gas phase. In this case, Q_t can be expressed by the equation

$$Q_t = \frac{t_{h^\cdot}}{F}\left[\bar{S}_{h^\cdot} + \frac{q^*_{h^\cdot}}{T}\right]_{p_{H_2O},p_{O_2}} + \frac{t_{H^+}}{2F} \times \left[RT\frac{d\ln K_{OX}K_H^2}{dT} - \frac{RT}{2}\Theta + 2\left(\bar{S}_{h^\cdot} + \frac{q_{H^+}}{T}\right)\right]_{p_{H_2O},p_{O_2}} - \frac{t_{O^{2-}}}{4F}\left[RT\cdot\Theta + \left(-4\bar{S}_{h^\cdot} + \frac{2q^*_{O^{2-}}}{T}\right)\right]_{p_{H_2O},p_{O_2}}, \quad (5)$$

where

$$\Theta = \left(\frac{\partial \ln P_{O_2}}{\partial \ln[V_O^{\cdot\cdot}]}\right)_{T,[H_i^\cdot]}\frac{d\ln[V_O^{\cdot\cdot}]}{dT} + \left(\frac{\partial \ln P_{O_2}}{\partial \ln[H_i^\cdot]}\right)_{T,[V_O^{\cdot\cdot}]}\frac{d\ln[H_i^\cdot]}{dT},$$

where q_j^* is the heat of transport of the respective carrier j, and $\bar{S}_{h^\cdot}$ ($= -R\ln(p/N_V)$) is the configurational partial molar entropy of holes. Solving Eq. (5) with (1)–(3), one can obtain the analytical equation for Q_t under wet conditions in terms of defect chemical properties (K_{OX}, K_H) and transport properties such as the mobility of the carriers and the heat of transport under given p_{O_2}, p_{H_2O}, and T without introducing assumptions.

From an examination of the experimental results using Eq. (5), both the electronic and ionic parts of the partial Seebeck coefficients were approximated to be proportional to the $-1/4$ power of p_{O_2} within experimental error. This is consistent with the analysis made on the Seebeck coefficient of proton-conducting $LaPO_4$ by Amezawa and Ratkje [8], but is different because the defect chemical reactions are taken into account. The total Seebeck coefficients are expressed in terms of partial Seebeck coefficients of ions (Q^o_{ion}) and holes (Q^o_p) at unit p_{O_2} using the following equations:

$$Q_t = t_{h^\cdot}\left(-\frac{R}{4F}\ln p_{O_2} + Q^o_p\right) + t_{ion}\left(-\frac{R}{4F}\ln p_{O_2} + Q^o_{ion}\right) \quad (6)$$

and

$$Q^o_p = \frac{R}{F}\left(\ln\frac{N_V}{p^o} + A_p\right), \quad (7)$$

where p^o, A_p, and N_V are the hole concentration at unit p_{O_2}, the density of state of the valence band, and the transport coefficient. As the hopping conduction of small polarons was the most probable mechanism for this system and the valence band is composed of the O2p orbital, we assume $A_p = 0$, $q^*_{h^\cdot} = 0$, and the value of N_V being equal to the concentration of oxide ions, in order to estimate p^o.

Eq. (6) can be rewritten in the extreme cases of (a) dry conditions, $[In'_{Zr}] \approx 2[V_O^{\cdot\cdot}] \gg p$, and (b) proton saturation conditions, $[In'_{Zr}] \approx [H_i] \gg [V_O^{\cdot\cdot}]$, p, as follows:

$$Q_t = \frac{t_{h^\cdot}}{F}\left[\bar{S}_{h^\cdot} + \frac{q^*_{h^\cdot}}{T}\right]_{p_{H_2O},p_{O_2}} - \frac{t_{O^{2-}}}{2F}\left[\frac{\Delta H_{OX}}{T} + \left(-2\bar{S}_{h^\cdot} + \frac{q^*_{O^{2-}}}{T}\right)\right]_{p_{H_2O},p_{O_2}}, \quad ([In'_{Zr}] \approx 2[V_O^{\cdot\cdot}] \gg p), \quad (8)$$

$$Q_t = \frac{t_{h^\cdot}}{F}\left[\bar{S}_{h^\cdot} + \frac{q_{h^\cdot}}{T}\right]_{p_{H_2O},p_{O_2}} + \frac{t_{H^+}}{F}\left[\frac{\Delta H_H}{T} + \left(\bar{S}_{h^\cdot} + \frac{q^*_{H^+}}{T}\right)\right]_{p_{H_2O},p_{O_2}}, \quad ([In'_{Zr}] \approx [H_i] \gg [V_O^{\cdot\cdot}],\ p). \quad (9)$$

A detailed discussion of the theoretical background will be published elsewhere [9].

3.2. Experimental results

Fig. 1 shows the total conductivity determined in the present study. The ionic conductivity, being independent of p_{O_2}, and hole conductivity in the higher p_{O_2} regime are clearly observed. The thick and thin dotted lines indicate the best fit results for the present (wet) and dry conditions, respectively. One can clearly observe the increase in ionic conductivity and decrease in hole conductivity under wet conditions in comparison with dry conditions at the same p_{O_2}.

Results for the total Seebeck coefficient are shown in Fig. 2 as a function of p_{O_2}. Q_t values decrease under the wet atmosphere in comparison with the dry

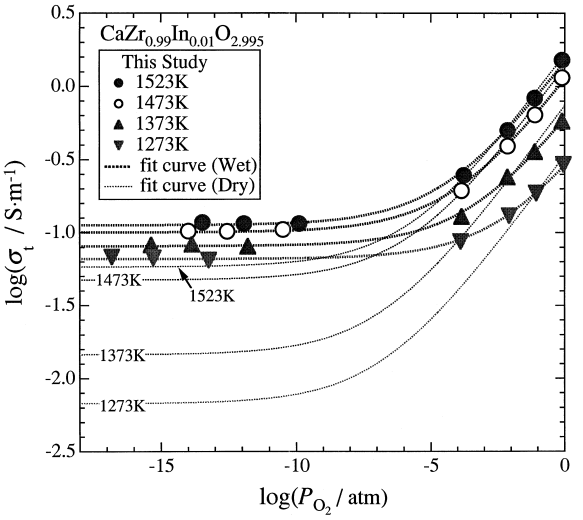

Fig. 1. Total conductivity of $CaZr_{0.99}In_{0.01}O_{2.995}$ under wet conditions ($P_{H_2O} = 0.037$ atm) as a function of $\log P_{O_2}$. The best fit curves for wet (thick lines) and dry conditions (thin dotted lines) [3] are plotted for comparison.

atmosphere because of the decrease in the contribution of holes. No reliable results could be obtained in the low-p_{O_2} region similar to those under dry conditions [3]. The thick and thin dotted broken lines show the fit results using the present approximation, showing good agreement with the experimental data.

3.3. Analysis of the electronic properties

Figs. 3 and 4 show the temperature variation of p^{o} and the mobility of holes (μ_p), respectively. In this calculation, we assumed that all the oxygen vacancy sites were equivalent and capable of being occupied. The values of p^{o} under the present wet conditions deviate from those under dry conditions at lower temperatures, but tend to agree at higher temperature due to the evolution of protons. The equilibrium constants for the quasi-chemical reactions were estimated by fitting data to Eqs. (1)–(3) and can be expressed as

$$K_{OX} = 4.20 \times 10^{-3} \exp(-68\,069\ [J]/RT), \quad (10)$$

$$K_{H} = 14.9 \times 10^{-3} \exp(112\,850\ [J]/RT). \quad (11)$$

The present results suggest that the concentration of protons saturates at about 1173 K under the present H_2O pressure ($p_{H_2O} = 0.037$ atm), in contrast to the

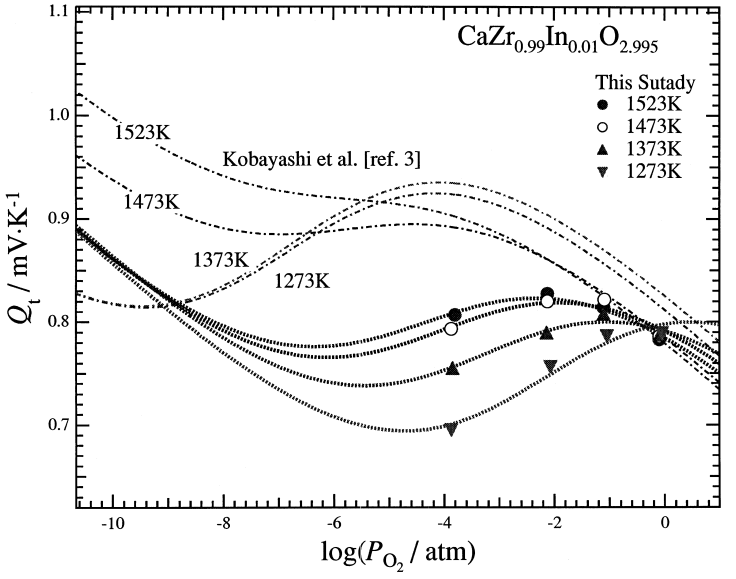

Fig. 2. Total Seebeck coefficient of $CaZr_{0.99}In_{0.01}O_{2.995}$ under wet conditions ($P_{H_2O} = 0.037$ atm) as a function of $\log P_{O_2}$. The best fit curves for wet (thick lines) and dry (thin dotted broken lines) [3] conditions are plotted for comparison.

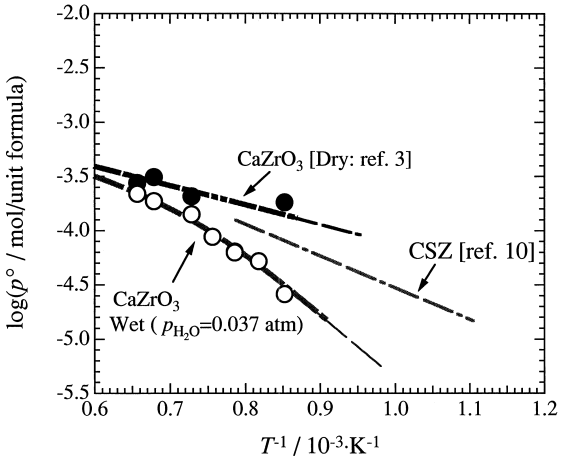

Fig. 3. Temperature variation of the concentration of holes at unit oxygen pressure under wet (○) and dry (●) [3] conditions. Result for CSZ [10] shown for comparison.

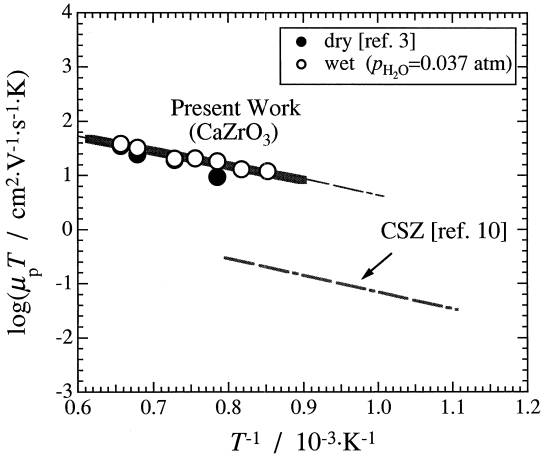

Fig. 4. Arrhenius plot of the mobility of holes. Result for CSZ [10] shown for comparison.

previous report on 10 mol% $InO_{1.5}$-doped $CaZrO_3$, in which the defect chemical parameters were estimated from the total conductivity measurements with the assumption that $[In'_{Zr}] \approx 2[V_O^{\cdot\cdot}] \gg p$ holds under humidified atmosphere. A preliminary experiment on the solubility of protons by off-line gravimetry was carried out in order to confirm the present analysis, showing that the weight change observed for the same sample annealed under different wet (1073 K, $P_{O_2} = 0.97$ atm, and $P_{H_2O} = 0.03$ atm) and dry (1473 K, $P_{O_2} = 0.97$ atm, and $P_{H_2O} = 0.03$ atm) conditions corresponds to one-third of the value expected for the full saturation of protons. Therefore, the authors conclude that the present estimation is reasonable.

Excellent agreement for μ_p under dry and wet conditions, calculated separately, also indicates the consistency of the present estimation. The activation energy for the mobility of holes was calculated as 0.53 eV. As this value is too large in comparison with the proposed range for the hopping conduction of small polarons, the authors suggest the presence of a hole trap, as described below.

3.4. Analysis of the ionic transport properties

Fig. 5 shows Arrhenius plots of the mobility of oxide ions and protons, calculated from the partial conductivity, transference number, and the concentrations of the respective carriers. The activation energy for the mobility of protons, calculated as 0.66 eV, showed good correspondence with typical values reported for proton mobility in perovskite proton conductors, ranging from 0.4 to 0.7 eV [11,12].

From the analysis of the ionic part of the Seebeck coefficient, one can estimate the heat of transport of ionic carriers from the plot of $Q^{\circ}_{ion} - Q^{\circ}_{p}$ versus $1/T$

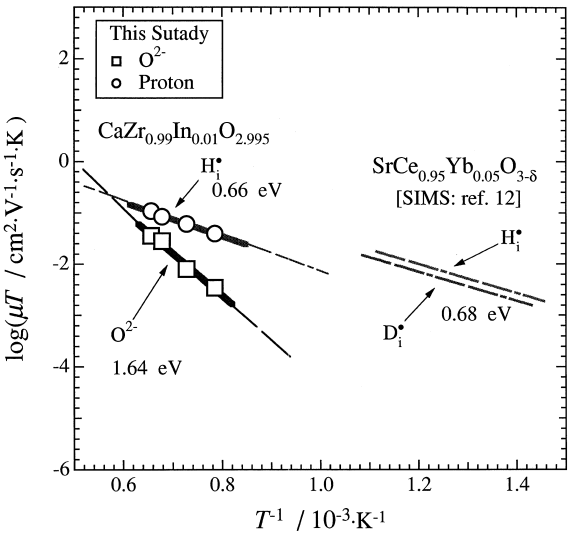

Fig. 5. Arrhenius plot of the mobility of protons and oxide ions. The mobility estimated by diffusivity measurements [12] is shown for comparison.

using the relationship obtained from Eqs. (8) and (9). Values of the heat of transport for oxide ions and protons estimated in the present study are 0.60 and 0.48 eV, respectively. The former value is far below the activation energy for the migration of oxide ions (1.64 eV). Since oxide ions migrate via a vacancy mechanism, it may not be necessary for them to coincide as proposed for substitutional alloys [13]. On the other hand, the heat of transport of protons showed fairly good agreement with the activation energy for the migration of protons (0.66 eV) as predicted for the interstitial diffusion mechanism.

3.5. XAS measurements

Results of XAS for 2 mol% $InO_{1.5}$-doped $CaZrO_3$ annealed at 1073 K in (a) dry and oxidizing (P_{O_2} = 1.0 atm), (b) wet and oxidizing ($P_{O_2} = 0.963$ atm, $P_{H_2O} = 0.037$ atm), and (c) dry and reducing ($P_{CO}/P_{CO_2} = 1.0$) atmospheres are shown in Fig. 6. O1s absorption spectra show the density of state of the unoccupied states. From the dipole selection rules, it is indicated that the O1s XAS spectra of $CaZrO_3$ correspond to the transition into O2p character hybridized into the unoccupied Zr4d states. In addition to the impurity levels, the peak shift due to the effect of the core potential makes identification of spectra difficult. As a detailed discussion will be published in a forthcoming report [5], only a brief and simple explanation is given here.

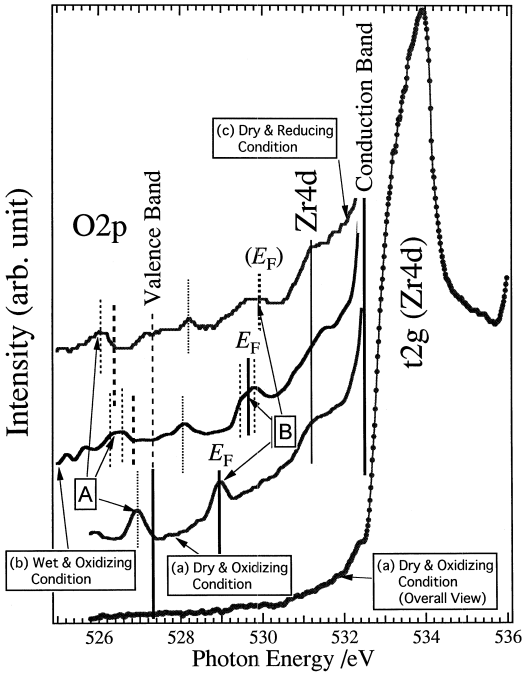

Fig. 6. O 1s X-ray absorption spectra of 2 mol% $InO_{1.5}$-doped $CaZrO_3$ annealed at 1073 K in (a) dry and oxidizing ($P_{O_2} = 10$ atm), (b) wet and oxidizing ($P_{H_2O} = 0.037$ atm, $P_{O_2} = 0.963$ atm), and (c) dry and reducing ($P_{CO}/P_{CO_2} = 1.0$) atmospheres.

The fundamental structure of $CaZrO_3$ is composed of the valence band of O2p and the conduction band of Zr4d. The top of the valence band is the nonbonding state of O2p, and the large density of state at the bottom of the conduction band corresponds to the t_{2g} state of Zr4d. Below the conduction band, a deformed Zr4d state created by the defect (oxygen vacancy) is observed. The e_g state of Zr4d located above the t_{2g} state is not shown in Fig. 6. Because of the selection rule for excitation, there is no absorption of the In5s state which is expected to be present in the middle of the band gap (possibly $\approx$3.5 eV above the top of the valence band).

The spectra of sample (a) show the presence of holes at the top of the valence band (O2p) termed feature A, but an analogous peak (feature B) is also observed at the Fermi level (E_F). Because feature B is always associated with the Fermi level, the authors suggest that feature B may reflect the surface levels. The hole concentration increases with increase of doped $InO_{1.5}$ content [5]. When protons dissolve, E_F shifts toward the conduction band side, and splitting of peaks is observed at both features A and B. The E_F shift is consistent with the decrease in the concentration of holes estimated from defect chemical calculations, and a further shift in sample (c) is expected. The splitting of the hole state is possibly caused by the formation of a new level, termed a proton-induced level, by the creation of an OH bond (hydrogen-bonded oxide ions) above the O2p band. A similar splitting by the formation of the proton-induced level has been observed in proton-dissolved $SrTiO_3$ [14]. When the sample was reduced, the peak intensity of features A and B decreased.

The authors suggest that the top of the valence band is composed of the defect-induced O2p level, which may be a localized state or an ensemble of defect-induced local bands, deformed by the pres-

ence of an oxygen vacancy. Taking into account the results of XAS, the authors suggest that the interpretation of the large activation energy for the migration of holes could be either the presence of an activation process of electrons from the O2p binding state to the trapping site of the defect-induced level or scattering by the deformation potential. As a strong and dopant-independent absorption of ≈ 1 eV is observed in ultraviolet absorption spectroscopy on $SrZrO_3$ samples doped with various kinds of lanthanide ions [15], the former seems a plausible interpretation.

4. Conclusion

The electronic transport properties and the electronic structure of 1 mol% $InO_{1.5}$-doped $CaZrO_3$ have been investigated by means of the simultaneous measurement of total conductivity and thermoelectric power and O1s X-ray absorption spectroscopy. Analyzing the results of the former technique, the authors deduced the defect chemical parameters for the annihilation of the oxygen vacancy and the dissolution reaction of protons. Through analyses of the ionic and electronic transport properties, mobilities of holes and protons, and oxide ions are obtained as well as the heat of transport of ionic species. The measurements of O1s X-ray absorption spectroscopy show consistent results with the defect chemical analysis.

References

[1] H. Iwahara, T. Esaka, H. Uchida, N. Maeda, Solid State Ionics 3/4 (1981) 359.
[2] N. Kurita, N. Fukatsu, K. Ito, T. Ohasi, J. Electrochem. Soc. 142 (1995) 1552.
[3] K. Kobayashi, S. Yamaguchi, Y. Iguchi, Solid State Ionics 108 (1998) 355.
[4] S. Yamaguchi, K. Kobayashi, Y. Iguchi, Solid State Ionics 113–115 (1998) 393.
[5] T. Higuchi, T. Tsukamoto, N. Sata, M. Ishigame, K. Kobayashi, S. Yamaguchi, Y. Ishiwata, T. Yokoya, M. Fujisawa, S. Shin, Solid State Ionics 136–137 (2000) 261.
[6] C. Wagner, Prog. Solid State Chem. 7 (1972) 1.
[7] H.-I. Yoo, J.-H. Hwang, J. Phys. Chem. Solids 53 (1992) 973.
[8] K. Amezawa, S.K. Ratkje, Denki Kagaku 64 (1996) 688.
[9] S. Yamaguchi, M. Takagi, K. Kobayashi, Y. Iguchi (in preparation).
[10] L. Heyne, N.M. Beekmans, Proc. Br. Ceram. Soc. 19 (1970) 229.
[11] T. Norby, Y. Larring, Curr. Opin. Solid State Mater. Sci. 2 (1977) 693.
[12] Y. Morita, Y. Yamazaki, Denki Kagaku 65 (1997) 663.
[13] P.G. Shewmon (Ed.), Diffusion in Solids, 2nd Edition, TMS, Warrendale, PA, 1989, p. 223.
[14] T. Higuchi, Unpublished.
[15] N. Sata, M. Ishigame, S. Shin, Solid State Ionics 86–88 (1996) 629.